BIOLOGY OF REPRODUCTION (2012) **86**(4):102, 1–9
Published online before print 21 December 2011.
DOI 10.1095/biolreprod.111.095216

Experimental Validation of *Ankrd17* and *Anapc10*, Two Novel Meiotic Genes Predicted by Computational Models in Mice[1]

Debjit Ray,[3,4,5] Cathryn A. Hogarth,[3,4] Elizabeth B. Evans,[3,4] Wenfeng An,[3,4] Michael D. Griswold,[3,4] and Ping Ye[2,3,4]

[3]*School of Molecular Biosciences, Washington State University, Pullman, Washington*
[4]*Center for Reproductive Biology, Washington State University, Pullman, Washington*
[5]*Biological Systems Engineering, Washington State University, Pullman, Washington*

ABSTRACT

Prophase is a critical stage of meiosis, during which recombination—the landmark event of meiosis—exchanges information between homologous chromosomes. The intractability of mammalian gonads has limited our knowledge on genes or interactions between genes during this key stage. Microarray profiling of gonads in both sexes has generated genome-scale information. However, the asynchronous development of germ cells and the mixed germ/somatic cell population complicate the use of this resource. To elucidate functional networks of meiotic prophase, we have integrated global gene expression with other genome-scale datasets either within or across species. Our computational approaches provide a comprehensive understanding of interactions between genes and can prioritize candidates for targeted experiments. Here, we examined two novel prophase genes predicted by computational models: *Ankrd17* and *Anapc10*. Their expression and localization were characterized in the developing mouse testis using in situ hybridization and immunofluorescence. We found ANKRD17 expression was predominantly restricted to pachytene spermatocytes and round spermatids. ANKRD17 was diffusely distributed throughout the nucleus of pachytene cells but excluded from the XY body and other heterochromatic regions. ANAPC10 was mainly expressed in the cytoplasm of spermatogonia and leptotene and pachytene spermatocytes. These experiments support our computational predictions of *Ankrd17* and *Anapc10* as potential prophase genes. More importantly, they serve as a proof of concept of our integrative computational and experimental approach, which has delivered a larger candidate gene set to the broader reproductive community.

Anapc10, Ankrd17, *computational model, experimental validation, genomics, germ cells, meiosis, prophase, spermatogenesis, testis*

INTRODUCTION

Meiosis is the highly conserved cell division program that results in the production of haploid gametes. Although germ cells in both testis and ovary initiate meiosis in response to the extrinsic inducer retinoic acid [1, 2], the putative checkpoint controls and timing differ between sexes [3–6]. The entire pool of oocytes enters meiosis synchronously during embryogenesis and arrests at the end of prophase I prior to birth. Following puberty, a cohort of oocytes resumes meiosis I and enters meiosis II during each ovulation cycle, resulting in the release of one mature egg; meiosis II is completed upon fertilization. In contrast, male meiosis occurs postnatally, continuously, and asynchronously to give rise to four spermatids, although the first wave of spermatogenesis proceeds in a relatively synchronous manner.

Mammalian meiosis is characterized by an extended prophase during which homologous chromosomes pair and undergo recombination. Recombination not only generates genetic diversity in offspring but also is critical to the successful completion of meiosis [7]. However, our understanding of mammalian prophase remains incomplete because of technical difficulties in studying it. No permanent germ cell line is available, isolated germ cells can be maintained in vitro for only a few days, and no reliable transfection procedure exists for isolated germ cells. Further, the initiation of female meiosis during fetal development hampers the retrieval of adequate amounts of ovarian tissue for analysis. Consequently, we know remarkably little about the process with the exception of a few well-characterized genes.

Genes involved in conserved processes such as recombination and chromosome behavior have been identified using tractable model systems and subsequent mapping for mammalian orthologs [4]. However, many genes required for mammalian meiosis have no ortholog in invertebrates. For instance, genes controlling meiotic entry in response to retinoic acid signaling are unique to mammals [1, 2]. Direct experimental approaches are therefore required to identify genes specific for mammalian meiotic prophase. Several critical prophase genes were originally linked to cancers and identified from mouse models with null mutations [8, 9]. More recently, unbiased genomic approaches have been employed for the discovery of novel meiotic genes. Random mutagenesis and phenotype screening for infertility increased the number of known meiotic genes [10–12]. Transcriptional profiling of mammalian gonads also helped to identify candidate genes for functional characterization [13–20] and has been particularly powerful when combined with conditional knockouts in embryonic stem cells [21].

However, the use of transcriptional profiling in gonads requires careful consideration of two issues: the asynchronous development of germ cells and the presence of both germ and somatic cells within the gonad. Although sorted germ cells can be obtained from males using physical separation methods, the limited amount of fetal ovarian tissue creates difficulty in

[1]Supported by March of Dimes Basil O'Connor Starter Scholar Research Award and Washington State University startup funds to P.Y. and National Institutes of Health grant HD10808 to M.G.
[2]Correspondence: Ping Ye, School of Molecular Biosciences, Washington State University, P.O. Box 647520, Pullman, WA 99164.
E-mail: pye@wsu.edu

Received: 29 July 2011.
First decision: 26 August 2011.
Accepted: 9 December 2011.

eISSN: 1529-7268 http://www.biolreprod.org
ISSN: 0006-3363

isolating germ cells from females. Further, acquiring human tissues is difficult for both sexes. Under these conditions, computational methods offer an essential complement for traditional approaches to decipher germ cell signals from gonad microarray profiles.

To date, most profiling studies have applied clustering methods to group genome-wide genes [13–20]. Such a strategy can identify hundreds of candidates, precluding prioritization for targeted mutagenesis. To circumvent this problem, we have pioneered network models to investigate genome-wide interactions between genes during meiotic prophase and predict candidates based on quantitative links with known meiotic genes, yielding a more manageable set of candidates [22, 23]. These two studies took advantage of gonad expression profiles in prophase of oogenesis and in the first wave of spermatogenesis, the most synchronized meiotic process. The goal of our first study was to delineate functional pathways of human fetal oogenesis [23]. We applied a naïve Bayesian network approach to integrating genome-scale datasets, including gene expression, protein interactions, disease phenotype, protein domain, phylogeny, and gene ontology. We calculated the joint likelihood ratio for gene pairs as a quantitative measure of functional associations. Connecting gene pairs with likelihood ratios greater than a threshold gives rise to a complex topological view of a network. This functional network of the human fetal ovary, HFOnet, provides a comprehensive understanding of interactions between genes in meiotic prophase. We demonstrated that the performance of the Bayesian method is better than the prediction based on any single genome-scale dataset. The advantage of this approach lies in the integration of heterogeneous datasets that leads to a high-confidence functional network.

Our second study focused on identifying evolutionarily conserved gene modules in meiotic prophase by integrating cross-species and cross-sex expression profiles in yeast, mouse, and human [22]. We defined metagenes as genes conserved across species; the use of metagenes allowed us to connect expression profiles across species. To identify conserved coexpression metagene pairs, we calculated *P* values according to the joint cumulative distribution of order statistics. Metagene pairs with *P* values greater than a threshold can be connected to form networks. Our approach greatly improved the identification of mammalian meiotic genes compared to an approach whereby the expression profile from a single species is used. We also demonstrated that conserved coexpression pairs exhibit functional connections, as evidenced by annotation similarity and overlap with physical interactions.

Our computational approaches are quantitative, i.e., a weight is assigned to each link between two genes in a network. These weighted networks allow us to prioritize candidates through their functional links or conserved coexpression links with known meiotic genes. We have conducted yeast sporulation assays to validate six candidates that exhibit conserved coexpression with known meiotic genes and found that deletion mutants of each of the six genes exhibited meiotic defects [22]. Here, we experimentally validated two novel genes—*Ankrd17* and *Anapc10*—in the mouse, both showing either functional or coexpression links with mismatch repair genes from our computational models [22, 23]. We examined mRNA expression and protein localization of these two genes in developing germ cells of mouse testis. Our results supported the prediction that these genes may play important roles in meiotic prophase. Meiotic function of these genes should be further characterized using mouse models with null mutations.

MATERIALS AND METHODS

Animals and Tissues

All animal procedures were approved by the Washington State University Animal Care and Use Committees. Washington State University is fully accredited by the American Association for Accreditation of Laboratory Animal Care. BL/6-129 mouse colonies were maintained in a temperature- and humidity-controlled environment. Drinking water and food were provided ad libitum. Male mice used in this study ranged from 5 to 90 days postpartum (dpp) and were euthanized by asphyxiation followed by cervical dissociation. Testis samples were collected and frozen immediately at −80°C for later protein extraction. Testis samples for in situ hybridization and immunofluorescence were collected and immediately placed in Bouin fixative for 5 h or 4% paraformaldehyde overnight. The samples were subsequently dehydrated with ethanol and embedded in paraffin. Tissue sections of 3–5 μm were placed on slides and stored at room temperature (RT) for future use. To capture most stages of meiotic prophase, 20-dpp testis samples were used to produce spermatocyte meiotic spreads using a published protocol [24]. Briefly, testes were collected and detunicated immediately. Tubules were physically separated and a small section of tubule was macerated in a sucrose solution to form a cell suspension. Cell suspension was spread across slides and dried overnight in a humidified chamber at 37°C. Embryos of both sexes at embryonic day 12.5 were dissected and frozen immediately at −80°C for later protein extraction.

In Situ Hybridization

In situ hybridization was performed to detect localization of mRNAs on cross sections of testis tissues. Locked Nucleic Acid (LNA) probes (Exiqon) were designed to either span exon-exon junctions or cover exon regions of a gene and to target the unique mRNA sequence of the gene. One digoxigenin (DIG) molecule was incorporated in the 5′ end of the LNA probe. Two probes were designed for *Ankrd17* detection: *exon1516*—5′TCCACTGA CTGCTGCCATGATGT and *3069*—5′TGGCTGTCCAACTATCACTCCT. Probe *exon1516* targets nucleotides 3200–3222 of NM_030886 and spans the exon 15-exon 16 junction. Probe *3069* targets nucleotides 3069–3090 of NM_030886 in exon15. As exon 15 (nucleotides 2459–3211 of NM_030886) is absent in the other isoform NM_198010, these two probes allow us to detect isoform-specific expression. Two probes were designed for *Anapc10* detection: *exon12*—5′ATGACAATCCTTCTGATTCGCCACA and *1661*—5′TAGCCTTCCATCCACCATAAGT. Probe *exon12* targets nucleotides 13–37 of NM_026904 and spans the exon 1-exon 2 junction. Probe *1661* targets nucleotides 1661–1682 of NM_026904 in exon 5. The negative scrambled probe is 5′GTGTAACACGTCTATACGCCCA.

The in situ procedure was based on a published protocol [25] with modifications. Briefly, Bouin-fixed tissue slides were used; tissue sections were digested with 1 μg/ml proteinase K (Roche) at 37°C for 30 min. Tissue slides were hybridized with 500 nM probes overnight at a desired temperature (45°C for *Ankrd17 exon1516*, 50°C for *Ankrd17 3069*, 48°C for both probes of *Anapc10*). An alkaline phosphatase-conjugated anti-DIG antibody (1:100; Roche) was applied to the slides at RT for 1 h. The mRNA expression was finally detected by incubating slides with nitro-blue tetrazolium chloride/5-bromo-4-chloro-3′ indolyphosphate p-toluidine salt solution (Roche). Harris hematoxylin (Sigma-Aldrich) was subsequently applied to stain nuclear chromatin. Tissue sections were digitally photographed using a Nikon Microphot-FX microscope. Testis tissues from at least three mice were analyzed for each gene probe; the negative probe was used in every experiment.

Western Blot Analysis

Testes and embryos were homogenized on ice to prepare protein samples in RIPA buffer (1% nonidet P-40, 0.5% sodium deoxycholate, 0.1% SDS in PBS) containing protease inhibitors (Roche). Proteins were extracted similarly from logarithmically growing mouse fibroblast NIH 3T3 cells and human embryonic kidney 293T cells. Protein concentration was measured using the DC protein assay kit (Bio-Rad). A 30-μg protein sample was loaded onto each lane of an SDS-PAGE gel. To detect ANKRD17, proteins were separated on a 6% gel with a high-range protein ladder (Thermo) and transferred to Protran nitrocellulose membrane (Whatman) at 4°C for 45 h. To detect ANAPC10, proteins were separated on a 15% gel with a protein ladder (Fermentas) and transferred to nitrocellulose membrane for 1 h. To ensure complete transfer of proteins to the membrane, the membrane was stained with Ponceau S solution (0.2% Ponceau S in 3% acetic acid) to detect proteins. Membranes were blocked in 5% nonfat dry milk TBS for 1 h. Incubation with primary antibodies (rabbit anti-ANKRD17 [1:1000; IHC-00596; Bethyl Laboratories], rabbit anti-ANKRD17 [1:1000; A301-664A; Bethyl Laboratories], rabbit anti-ANAPC10 [1:1000; sc20989; Santa Cruz Biotechnology], mouse anti-β-actin [1:5000;

A5316; Sigma]) was performed at 4°C overnight. The peptide blocking experiment was conducted by incubation with both rabbit anti-ANKRD17 (1:1000; A301-664A and IHC-00596) and the peptide (1:200; BP301-664; Bethyl Laboratories) that specifically blocks the ability of A301-664A to bind ANKRD17. Incubation with horseradish peroxidase-coupled secondary antibodies (anti-rabbit [1:5000; GE Healthcare], anti-mouse [1:5000; GE Healthcare]) was performed at RT for 1 h. Protein signals were visualized using the ECL Western blotting system (GE Healthcare). Membranes were digitally photographed using LAS 4000 (Fujifilm). Each primary antibody was tested on at least two distinct protein homogenates for each tissue type or cell line.

Immunofluorescence

The immunofluorescence procedure was based on a published protocol [25] with modifications. The primary antibodies utilized in Western blots were applied to testis sections to examine protein localization by immunofluorescence. ANKRD17 and ANAPC10 were detected using Bouin-fixed and paraformaldehyde-fixed testis sections, respectively. Tissue slides were boiled in 0.01 M citrate buffer (pH 6) for 5 min to retrieve antigens. Tissue sections were blocked with 10% normal goat serum for 30 min and incubated with either rabbit anti-ANKRD17 (1:1000; IHC-00596; Bethyl Laboratories) or rabbit anti-ANAPC10 (1:200; sc20989) at RT overnight. Tissue sections were subsequently incubated with Alexa Fluor 488 goat anti-rabbit IgG (1:1000; Invitrogen) at RT for 1 h to detect rabbit anti-ANKRD17, or with biotin-SP conjugated goat anti-rabbit IgG (1:500; Millipore) followed by Alexa Fluor 488-conjugated streptavidin (1:1000; Invitrogen), both at RT for 1 h, to detect rabbit anti-ANAPC10. Tissue slides stained for both ANKRD17 and ANAPC10 were mounted under coverslips using Vectashield with 4′,6-diamidino-2-phenylindole (DAPI; Vector Laboratories). Tissue sections were digitally photographed using a Zeiss Axioplan microscope. Control experiments followed the same procedure except incubation was without the primary antibody. Tissue sections from at least three mice were analyzed for each immunofluorescence experiment.

Spermatocyte Meiotic Spread

Spermatocyte spreads were immunostained similarly to testis sections in the immunofluorescence experiment. Cells were blocked with 10% normal donkey serum for 30 min and subsequently incubated with rabbit anti-ANKRD17 (1:200; IHC-00596) overnight followed by goat anti-SYCP3 (1:75; sc33874; Santa Cruz Biotechnology) for 2 h, both at 37°C. After two washes, cells were incubated with Alexa Fluor 488 donkey anti-rabbit IgG (1:75; Invitrogen) overnight followed by Alexa Fluor 568 donkey anti-goat IgG (1:200; Invitrogen) for 45 min, both at 37°C. Slides were mounted using Vectashield with DAPI (Vector Laboratories) and visualized under a Zeiss Axioplan microscope. Control experiments followed the same procedure except incubation was without anti-ANKRD17 or anti-SYCP3. The spermatocyte spread experiment was repeated on cells from at least three mice.

RESULTS

Developmental Expression and Localization of Ankrd17

Identification of Ankrd17 *as a candidate prophase gene.* *Ankrd17* stands for ankyrin repeat domain-containing protein 17. In our functional gene network of human fetal ovary, *ANKRD17* forms a clique with DNA mismatch repair genes *MSH4*, *MSH5*, and *MSH3* [23]. A clique is a set of genes in which each one is connected to every other, providing a stringent definition for meiotic functional pathways. This result indicates that ANKRD17 might function in prophase although this protein has never been implicated in the meiotic process. Interestingly, *Ankrd17* is expressed in fetal ovary and adult testis in both human and mouse [14, 16, 19, 20, 26]. It is induced in embryonic stem cells treated with retinoic acid [27]. Further, *ANKRD17* exhibits an expression pattern similar to mismatch genes *MSH3*, *MSH4*, and *MSH5* in colorectal tumor samples [28]. These data support our prediction that *Ankrd17* has a possible role in meiosis and mismatch repair response. However, cellular expression patterns of *Ankrd17* were uncharacterized in the testis or ovary, neither its function in meiosis. We therefore examined mRNA and protein expression of *Ankrd17* in the developing mouse testis.

Ankrd17 *mRNA is expressed in multiple stages of male germ cells.* Two major mRNA isoforms of mouse *Ankrd17* are annotated in NCBI Reference Sequences (Build 37.2). The full-length *Ankrd17* mRNA (NM_030886) is 10 066 nucleotides long, containing 34 exons. Exon 15 is absent in the other isoform, NM_198010, which is 9313 nucleotides long with 33 exons. We designed two LNA probes that are uniquely mapped to *Ankrd17* mRNA. Probe *exon1516* covers the exon 15-exon 16 junction and probe *3069* targets exon 15. This probe design allows us to detect isoform-specific expression in the testis.

In situ hybridization was performed to determine the *Ankrd17* mRNA expression in cross sections of testis from 5-, 10-, 20-, and 90-dpp mice. Germ and somatic cell types were identified based on their nuclear morphology and position within the developing gonad. We observed that *Ankrd17* is constitutively expressed in germ cells from 5 to 90 dpp. Transcript was present in both cytoplasm and nuclei of germ cells. No expression was observed in Sertoli cells or the interstitial space between tubules at any age tested. Transcripts were mainly confined to spermatogonia at 5–10 dpp, with expression also detected in preleptotene and leptotene spermatocytes at 10 dpp (Fig. 1, B and C). At 20 and 90 dpp, pachytene spermatocytes exhibited the strongest *Ankrd17* signal; other stages of germ cells, specifically spermatogonia, preleptotene and leptotene spermatocytes, and round and elongating spermatids, also expressed the mRNA at these ages (Fig. 1, D–F). Images using *exon1516* are shown in Figure 1; hybridization with probe *3069* exhibited similar results. This suggests that the full-length *Ankrd17* mRNA (NM_030886) is present in the testis.

ANKRD17 protein is expressed in the testis. Two major protein isoforms of mouse ANKRD17 are also annotated in NCBI Reference Sequences (Build 37.2). The full-length protein (NP_112148) has 2603 amino acids with a predicted molecular mass of 274 kDa. It contains 25 ankyrin repeats and one KH domain; ankyrin repeats are among the most common sequence motifs that function as interaction mediators [29]. The other isoform (NP_932127) has 2352 amino acids with a predicted molecular mass of 247 kDa.

Before examining ANKRD17 expression in male germ cells, we first verified the specificity of commercial antibodies by Western blots using total testis protein extracts. Total lysates of mouse embryos and human 293T cells served as positive control because endogenous expression of ANKRD17 was detected in these controls at a molecular mass of ~260 kDa [30, 31]. We further included mouse 3T3 cells in the experiment. Both antibody IHC-00596 and antibody A301-664A recognize an epitope that maps to a region between residues 1550 and 1600 of human ANKRD17; this region exhibits 100% sequence identity to that of mouse ANKRD17. IHC-00596 is recommended for immunohistochemistry, whereas A301-664A is recommended for immunoprecipitation. Using A301-664A for Western blots, we identified two bands around 250 kDa in the positive control: embryos and 293T cells. We estimate that these two bands correspond to the isoforms of 274 and 247 kDa, confirming the specificity of the commercial antibody. Two bands around 250 kDa were also observed in 90-dpp testes and mouse cell line 3T3, but were absent from 10-dpp testes (Fig. 2A). Because most germ cells are spermatogonia at 10 dpp and are spermatids and spermatocytes at 90 dpp [32], the Western results suggest that spermatids and spermatocytes may exhibit stronger expression of ANKRD17 than spermatogonia. In addition, A301-664A recognized a few lower-molecular mass bands at 100 and 70 kDa, which may correspond to degraded proteins or short isoforms.

To further probe the specificity of ANKRD17 antibodies, we repeated Western blots in the presence of BP301-664, a

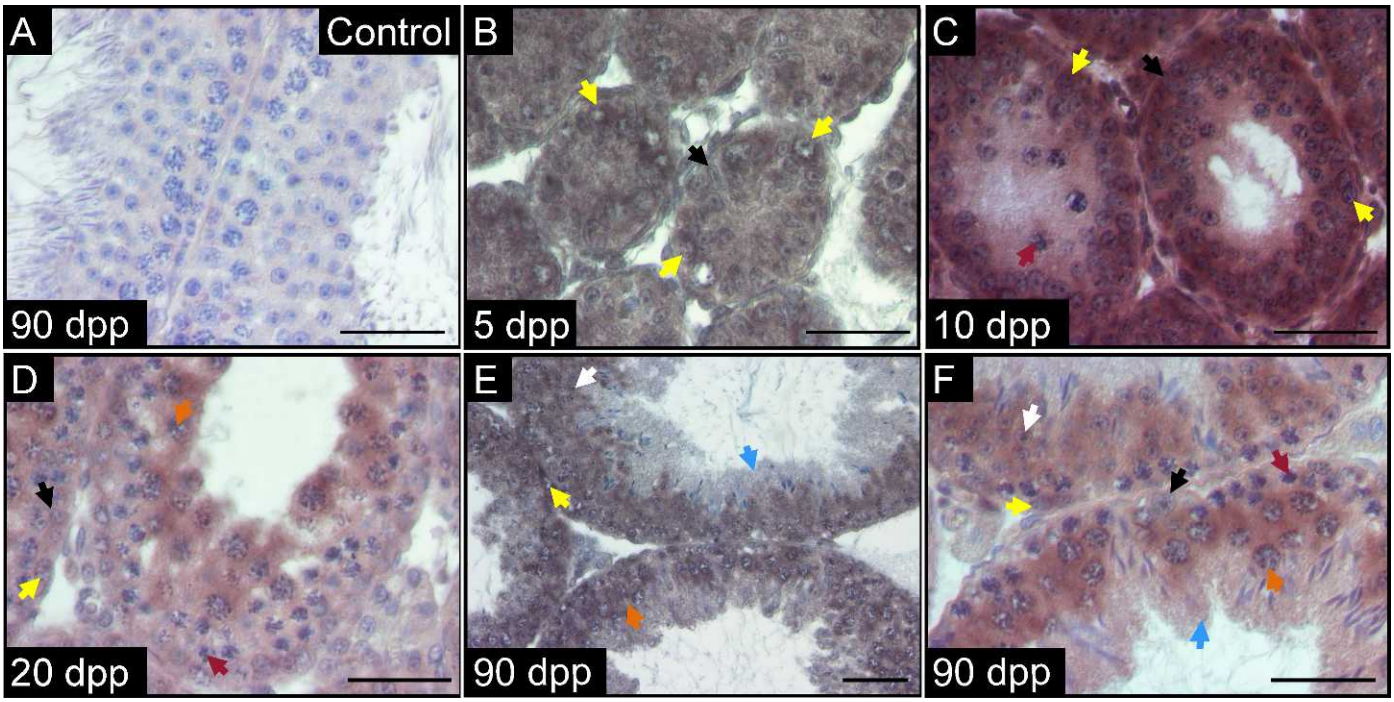

FIG. 1. *Ankrd17* expression in developing mouse testis. In situ hybridization was performed on testis cross sections using DIG-labeled LNA probes. Control section was hybridized to the negative scrambled probe (**A**). Cells with positive signal to *Ankrd17* probes are colored mauve (**B**–**F**). Chromatin is stained blue with Harris hematoxylin. Bars = 50 μm. Arrows: yellow, spermatogonia; red, preleptotene/leptotene spermatocytes; orange, pachytene spermatocytes; white, round spermatids; blue, elongating spermatids; black, Sertoli cells.

peptide that specifically blocks the ability of A301-664A to bind ANKRD17. No signal was detected in any sample (Supplemental Fig. S1; all Supplemental Data are available online at www.biolreprod.org), suggesting all bands observed in the Western blot without the blocking peptide are specific to ANKRD17 antibody. Western blots with antibody IHC-00596 in the absence and presence of the same blocking peptide exhibited similar results to those using A301-664A (Supplemental Fig. S2). These experiments confirmed the specificity of commercial antibodies A301-664A and IHC-00596. Thus IHC-00596 was used for all immunofluorescence experiments described below.

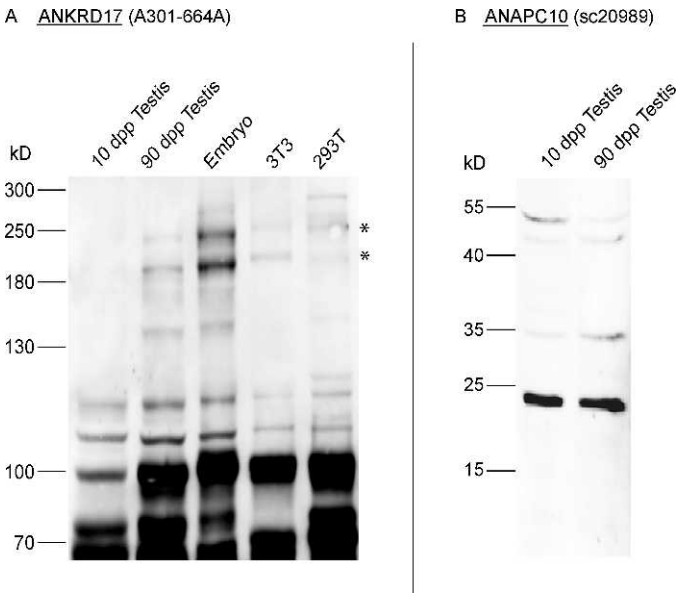

FIG. 2. Detection of ANKRD17 and ANAPC10 in mouse tissues and cell lines by Western blot analyses. Total protein lysates were prepared from 10- and 90-dpp testes, embryos at Embryonic Day 12.5, and 3T3 and 293T cells. ANKRD17 antibody (**A**) and ANAPC10 antibody (**B**) were used to detect protein expression. The asterisks in **A** mark the two bands around 250 kDa.

ANKRD17 protein localizes to the nucleus of male germ cells. Immunofluorescence experiments were performed to determine ANKRD17 localization within testis cross sections (Fig. 3). An age series of testis sections was examined in a similar manner to what was performed for in situ hybridization: 5, 10, 20, 30, and 90 dpp. Protein signals were mainly localized to the nuclei of spermatocytes, although granules of stain appeared in the cytoplasm of Sertoli cells at 5–10 dpp (Fig. 3, B and C). ANKRD17 expression first appeared in spermatogonia at 10 dpp (Fig. 3C). Diffuse staining was observed throughout the nuclei of pachytene spermatocytes from 20 to 90 dpp (Fig. 3, D–F). Round spermatids exhibited intense signals for ANKRD17 at 30 and 90 dpp (Fig. 3, E and F). Much stronger expression was observed in pachytene spermatocytes and round spermatids at 90 dpp than that in spermatogonia at 10 dpp. These results are consistent with our Western blot analyses, as we detected ANKRD17 (~250 kDa) in 90-dpp testes (mostly spermatids followed by spermatocytes) but not in 10-dpp testes (mostly spermatogonia) (Fig. 2A). Sertoli cells in older mouse tissues and the interstitial space between tubules showed no detectable expression of the protein. Protein localization of ANKRD17 was similar to mRNA expression patterns (Fig. 1), but with a time delay.

ANKRD17 protein localizes to euchromatin at the pachytene stage. Immunofluorescence experiments on testis sections suggest nuclear localization of ANKRD17 in spermatocytes. To determine whether ANKRD17 localizes to meiotic chromosomes, we performed immunostaining of spermatocyte spreads with anti-ANKRD17 and anti-SYCP3.

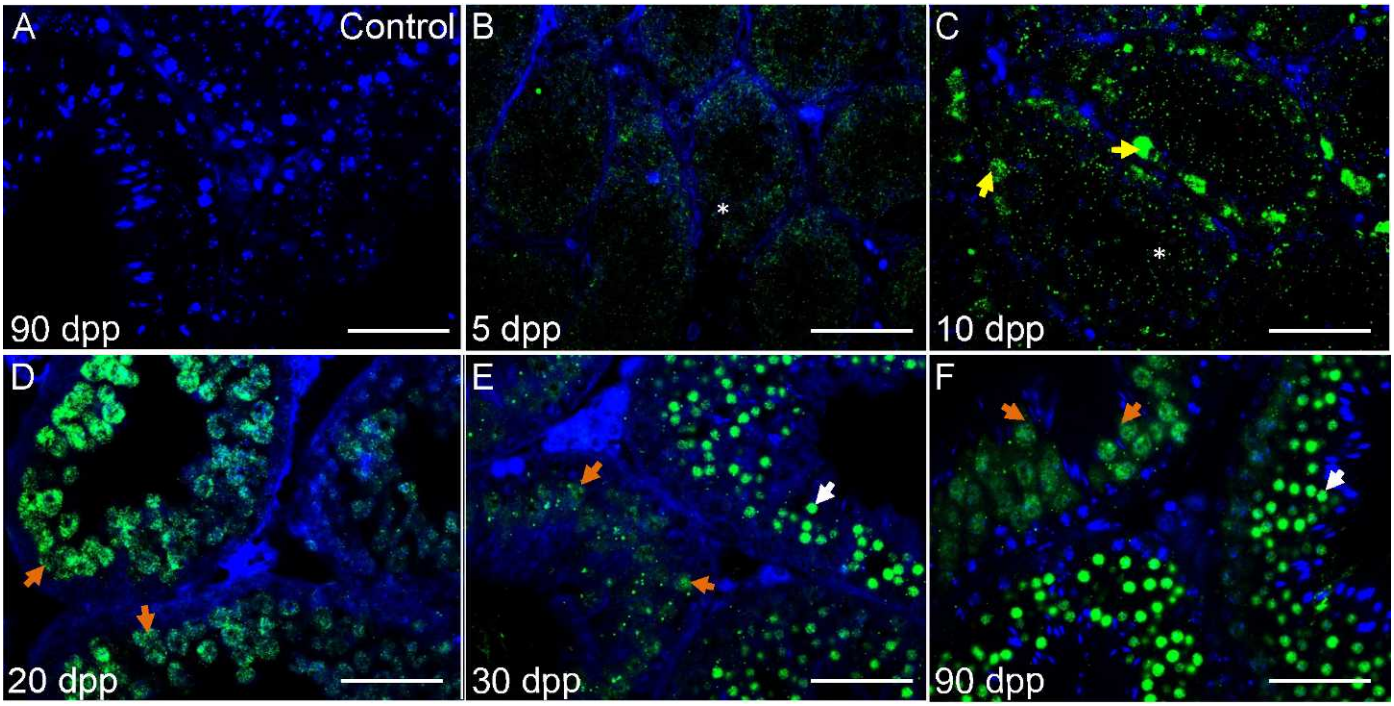

FIG. 3. Localization of ANKRD17 in developing mouse testis. Immunofluorescence was performed on testis cross sections. No anti-ANKRD17 serves as the control (**A**). ANKRD17 expression is colored green (**B**–**F**). DNA is stained blue with DAPI. Bars = 50 μm. Arrows: yellow, spermatogonia; orange, pachytene spermatocytes; white, round spermatids. Asterisks in **B** and **C** indicate cytoplasm of Sertoli cells.

We examined protein localization in four stages of meiotic prophase: leptotene, zygotene, pachytene, and diplotene (Fig. 4). ANKRD17 was absent at the leptotene stage and exhibited weak signals at the zygotene stage. Expression of ANKRD17 was strongest in pachytene cells and less intense in diplotene cells. The high expression of ANKRD17 in pachytene cells is consistent with its expression pattern within testis cross sections. Interestingly, although ANKRD17 was diffusely distributed across the nucleus during the pachytene and diplotene stages, it was absent from the XY body, a highly heterochromatic region where both transcription and recombination are restricted. Further, ANKRD17 was absent from areas with the most dense DAPI staining, also a hallmark of heterochromatin, particularly centromeres. These results suggest that ANKRD17 may associate only with euchromatin, potentially for regulating transcription and recombination. The localization of ANKRD17 onto euchromatin is also observed in round spermatids (Supplemental Fig. S3). No colocalization was observed between ANKRD17 and SYCP3, a marker for the synaptonemal complex between paired homologues.

Developmental Expression and Localization of Anapc10

Identification of Anapc10 *as a candidate prophase gene.* Anaphase-promoting complex (APC) is a conserved ubiquitin ligase complex that degrades mitotic cyclins and anaphase inhibitory proteins; it is required for anaphase initiation and mitotic exit [33–36]. APC activity is also important for the metaphase to anaphase transitions in meiosis, where cell division occurs twice [37]. ANAPC10 is an essential subunit of APC conserved from yeast to human [33–36]. In our conserved coexpression networks of meiotic prophase, *Anapc10* exhibits similar expression to *Msh4*, *Msh5*, and *Nipbl*, suggesting that *Anapc10* may also function in meiotic prophase [22]. Thus, we conducted sporulation experiments to validate the meiotic function of *DOC1*, the budding yeast ortholog of *Anapc10*. A deletion mutant strain of *doc1* exhibited more than 6-fold reductions in sporulation efficiency compared to wild type, and no tetranucleate cell was observed in the mutant [22]. This result is consistent with the sterile phenotype of the *apc10* mutant in fission yeast [36]. However, the sterile phenotype does not imply the timing of *Anapc10* function, which may occur in prophase or anaphase. The involvement of *Anapc10* in meiotic prophase has never been examined before. We know only that the *Anapc10* transcript was most abundant in the testis among several adult mouse tissues [38]. Therefore, we examined the cellular expression and localization of *Anapc10* within the testis using methods as for *Ankrd17*.

Anapc10 *mRNA is expressed in multiple stages of male germ cells.* *Anapc10* mRNA (NM_026904) is 2802 nucleotides long, containing five exons. We designed two LNA probes that uniquely target *Anapc10* mRNA. Probe *exon12* covers the exon 1-exon 2 junction and probe *1661* is complementary to exon 5. To determine *Anapc10* expression in an age series of testis sections, we performed in situ hybridization using these LNA probes. At each age examined from 5 dpp to adult, *Anapc10* transcripts localize specifically to the germ cell, mainly the cytoplasm. Expression was never detected in either Sertoli cells or the interstitial space. Spermatogonia showed the strongest signal for *Anapc10* among all germ cell types at every age. *Anapc10* initially appeared in spermatogonia at 5 dpp, then localized in both spermatogonia and preleptotene/leptotene spermatocytes from 10 dpp through adult (Fig. 5, B–F). Expression in pachytene spermatocytes began at 20 dpp; expression was present in round spermatids in adult testis sections (Fig. 5, D–F). Similar results were obtained from both probes, and images of hybridization with *exon12* are shown in Figure 5.

ANAPC10 protein is present in multiple stages of male germ cells. In contrast to ANKRD17, mouse ANAPC10 is a small one-domain protein consisting of 185 amino acids. The commercial antibody, sc-20989, was raised against full-length

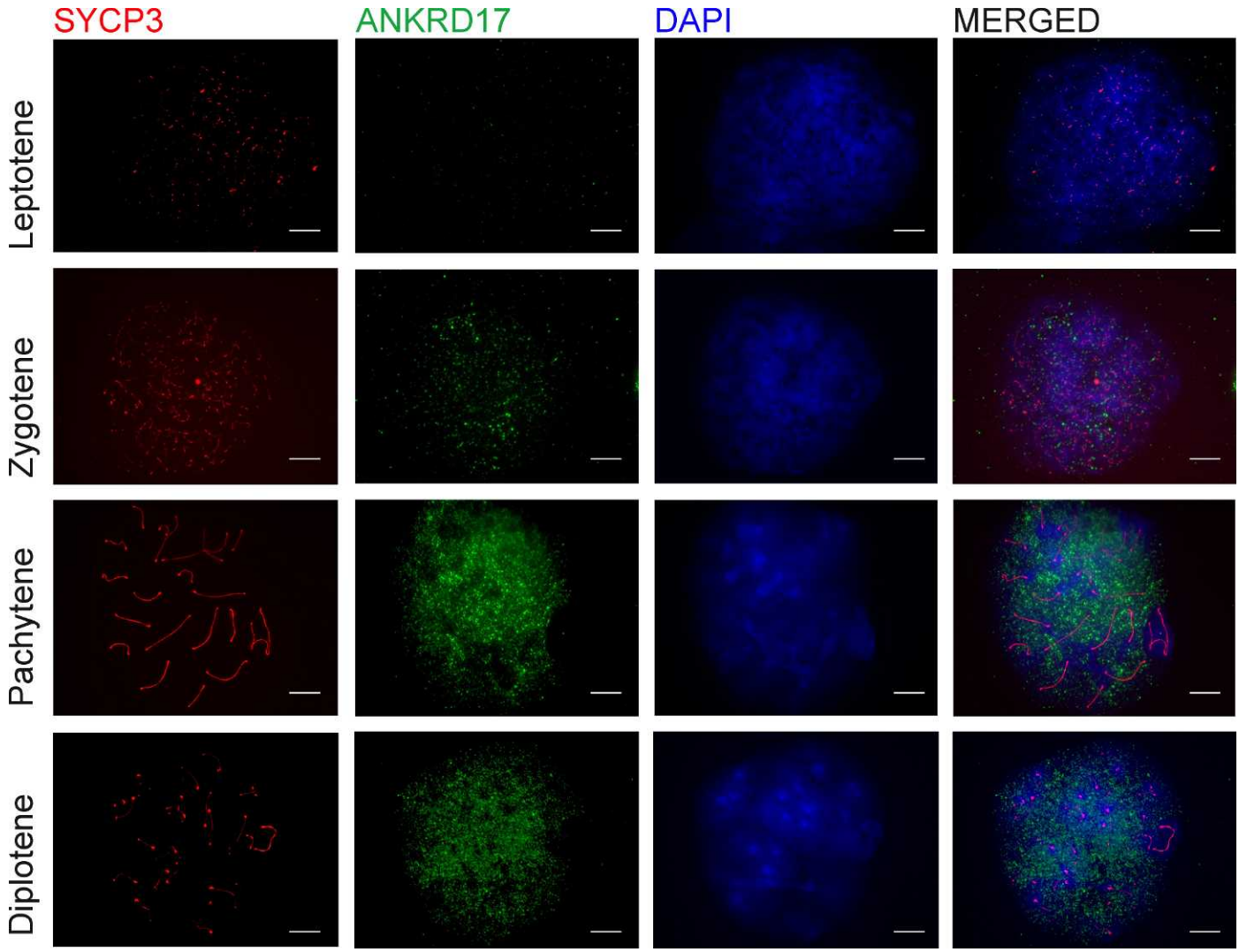

FIG. 4. Localization of ANKRD17 in meiotic cells. Immunofluorescence was performed on spermatocyte spreads from 20-dpp testes. ANKRD17 is colored green; SYCP3 is colored red; DNA is stained blue with DAPI. Four prophase stages were captured: leptotene, zygotene, pachytene, and diplotene. Bars = 10 μm.

human ANAPC10, which has 99% sequence identity to the mouse ortholog. The molecular mass of mouse ANAPC10 is predicted to be 21 kDa. One single band of the expected molecular mass was found in both 10- and 90-dpp testis samples by Western blotting, indicating that this antibody could specifically recognize ANAPC10 (Fig. 2C). A few weak bands with higher molecular masses were also detected, which could be because of association of ANAPC10 with other subunits in the APC complex or unidentified ligands [33, 39]. The specificity of the ANAPC10 antibody was further confirmed by detecting a specific band of 21 kDa in both nontransfected and mouse *Anapc10*-transfected 293T cells (Supplemental Fig. S4).

Cellular localization of ANAPC10 protein examined by immunofluorescence matched its mRNA expression by in situ hybridization. ANAPC10 localized to mitotic and meiotic germ cells, including spermatogonia, preleptotene/leptotene spermatocytes, and pachytene spermatocytes (Fig. 6). However, no signal was detected in round and elongated spermatids. Signal intensity was highest in the cytoplasm of germ cells. No nuclear expression was detected in cross sections or in spermatocyte spreads (data not shown). ANAPC10 exhibited diffuse signals in the cytoplasm of spermatogonia and Sertoli cells at 5 dpp but became restricted to germ cells as the animal matured (Fig. 6B). At 10 dpp, ANAPC10 was detectable in the cytoplasm of spermatogonia and preleptotene spermatocytes (Fig. 6C). At 20 dpp, ANAPC10 was present in leptotene and pachytene spermatocytes (Fig. 6D). From 30 dpp onwards, protein expression was confined to spermatogonia and preleptotene and pachytene spermatocytes (Fig. 6, E and F). No expression of ANAPC10 was detected in the interstitium or in Sertoli cells from 10 dpp onwards.

DISCUSSION

Meiosis is a developmental program essential for human reproduction. Indeed, meiotic errors are associated with infertility, miscarriages, and birth defects [40]. However, because of the intractability of mammalian gonads, we know remarkably little about genes or interactions between genes required for meiosis. We have developed computational models to investigate networks of meiotic prophase by integrating genome-scale datasets within or across species [22, 23, 41]. These quantitative approaches allow us to infer potential functional connections between genes and prioritize candidates for experimental testing. This study investigated the

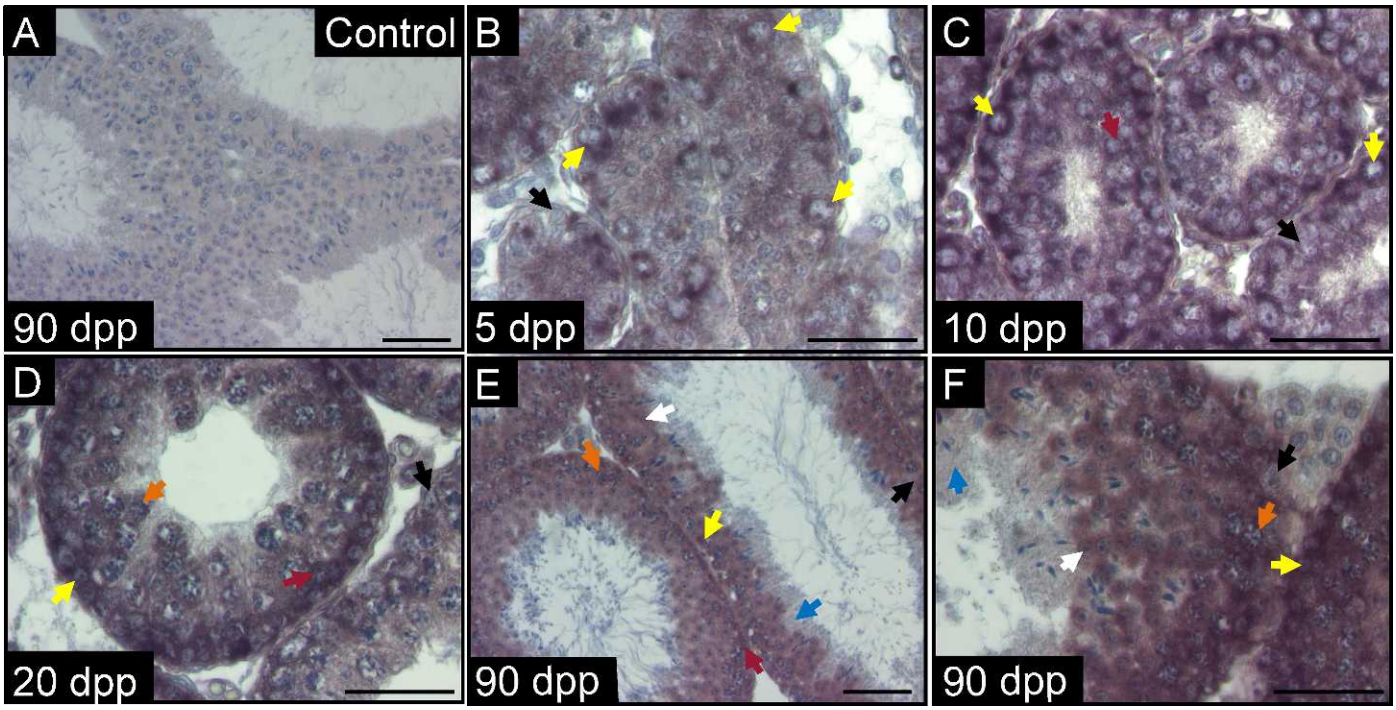

FIG. 5. *Anapc10* expression in developing mouse testis. In situ hybridization was performed on testis cross sections using DIG-labeled LNA probes. Control section was hybridized to the negative scrambled probe (**A**). Cells with positive signal to *Anapc10* probes are colored mauve (**B**–**F**). Chromatin is stained blue with Harris hematoxylin. Bars = 50 μm. Arrows: yellow, spermatogonia; red, preleptotene/leptotene spermatocytes; orange, pachytene spermatocytes; white, round spermatids; blue, elongating spermatids; black, Sertoli cells.

expression and localization of two candidate genes, *Ankrd17* and *Anapc10*, in the germ cell of developing mouse testes; both were identified from our computational networks of meiotic prophase.

Ankrd17 was initially cloned and identified from a gene trap integration in embryonic stem cells [27]. Interestingly, the expression of this gene trap cell line was induced after exposure to exogenous retinoic acid, suggesting *Ankrd17* is a

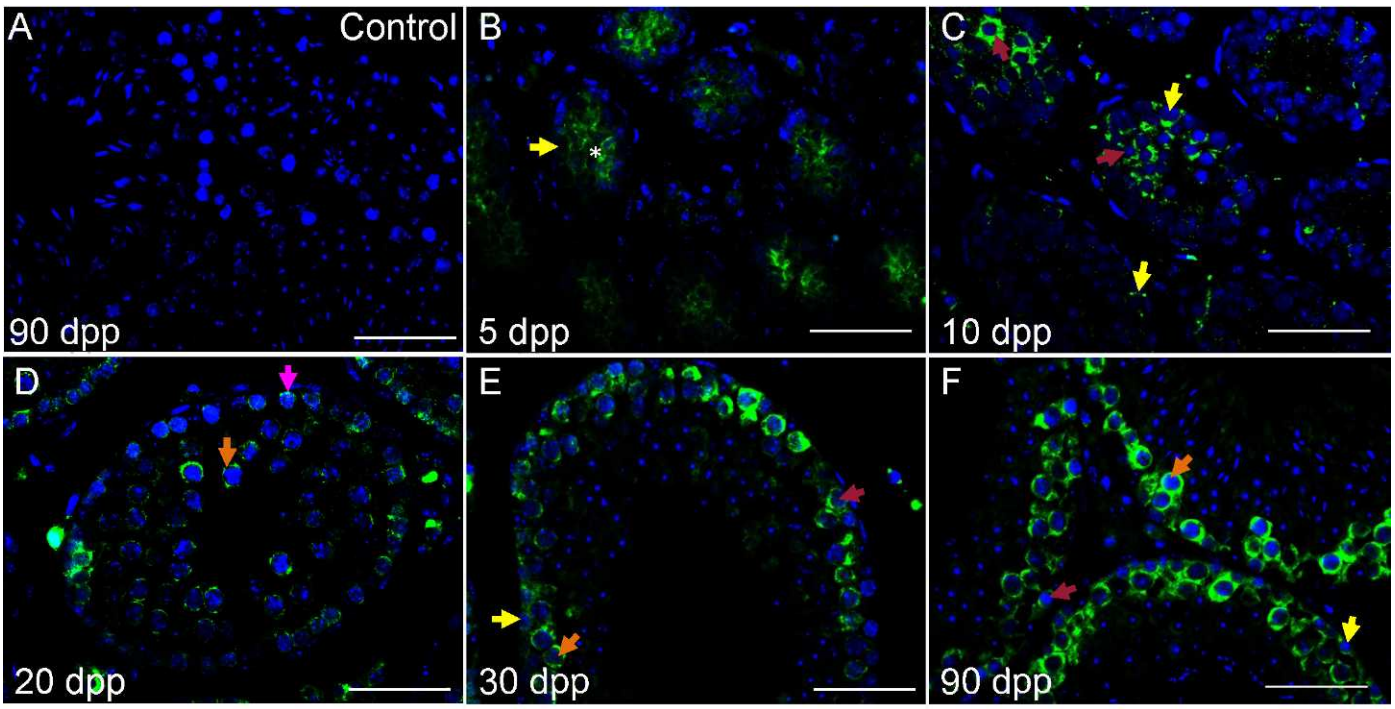

FIG. 6. Localization of ANAPC10 in developing mouse testis. Immunofluorescence was performed on testis cross sections. No anti-ANAPC10 serves as the control (**A**). ANAPC10 expression is colored green (**B**–**F**). DNA is stained blue with DAPI. Bars = 50 μm. Arrows: yellow, spermatogonia; red, preleptotene spermatocytes; pink, leptotene spermatocytes; orange, pachytene spermatocytes. Asterisk in **B** indicates cytoplasm of Sertoli cells.

retinoic acid-responsive gene [27]. Characterization of the mouse line with integration of the same gene trap indicates that *Ankrd17* is the earliest and most specific marker of fetal hepatic differentiation [26]. *Ankrd17*-deficient mice die prenatally because of cardiovascular defects [31]. Later cell culture studies identified *ANKRD17* as a substrate of cyclin E/CDK2 [30]. Overexpression of *ANKRD17* promotes S phase entry, whereas depletion of *ANKRD17* inhibits DNA replication and blocks cell cycle progression, suggesting its positive role in regulating G1-S transition [30]. Cell culture studies have also localized ANKRD17 to the nucleus and found it interacts with DNA replication factors as well as the VP1 capsid structural protein of enterovirus 71 [30, 42]. *Ankrd17* is ubiquitously expressed in a range of adult and fetal tissues in both human and mouse [16, 26, 30] and is also detected in fetal ovary and adult testis when meiosis occurs [14, 16, 19, 20, 26]. Further, expression of *ANKRD17* is reduced in colorectal tumor samples compared with the normal tissue, a pattern similar to mismatch repair genes such as *MSH3*, *MSH4*, and *MSH5* [28].

Despite these studies, it remained unknown whether *Ankrd17* functions in meiotic prophase. Our study represents the first investigation of *Ankrd17* expression and localization in the male germ cell. We found that the mRNA and protein expression patterns were concordant at different stages of testis development. ANKRD17 was prominently confined to the germ cell, particularly to pachytene spermatocytes and round spermatids. ANKRD17 was present only in the nucleus of the meiotic germ cells, which is consistent with its localization in somatic cells [30, 42]. Data from spermatocyte spreads confirmed that ANKRD17 was predominantly expressed at the pachytene stage. ANKRD17 was diffusely distributed across the nucleus but was absent from the XY body and other heterochromatic regions. The association of ANKRD17 with euchromatin of pachytene cells suggests its possible roles in regulating transcription or as a scaffold protein. Although our computational model suggests a potential role of ANKRD17 in meiotic recombination, this protein may not be directly involved in processing meiotic double strand breaks because it does not form foci associated with the synaptonemal complex. Thus the role of ANKRD17 in recombination is likely indirect.

APC is a multi-protein complex that functions as an ubiquitin ligase. APC initiates sister chromatid separation by ubiquitinating anaphase inhibitors, thus triggering mitotic exit [43]. APC activity is also essential for metaphase to anaphase transitions in both meiosis I and meiosis II [37]. Several studies have demonstrated the requirement of APC for homologue disjunction in meiosis I of mouse oocytes [44–46]. APC is composed of more than 10 subunits, most of which are conserved from yeast to vertebrates [33–36]. *DOC1*/*Anapc10* is a component of APC and is essential for APC function in both yeast and mouse [33–36]. Mutation of yeast *doc1* inactivates APC function [34], and a homozygous mutation in mouse *Anapc10* results in embryonic lethality [38, 47]. Both are due to mitotic arrest in the transition from metaphase to anaphase. In addition, *apc10* mutants in budding yeast and fission yeast exhibit sporulation defects [22, 36]. Structural studies suggest that APC10 confers substrate specificity by forming the receptor for destruction signals such as degrons [33, 48]. Human ANAPC10 is diffusely distributed in the cytoplasm throughout mitosis; additionally, ANAPC10 localizes in centrosomes, mitotic spindles, and kinetochores [39]. *Anapc10* is present in a variety of mouse tissues including liver, heart, spleen, and lung, but is strongest in the testis [38].

Until now it was thought that APC only functions during metaphase to anaphase transitions in meiosis. Our study suggests that *Anapc10* may act very early in meiotic prophase. ANAPC10 was mainly present in spermatogonia and leptotene and pachytene spermatocytes. More specifically, ANAPC10 localizes to the cytoplasm of germ cells, consistent with its subcellular localization in somatic cells during mitosis [39]. This suggests that ANAPC10 may play a role in remodeling the cytoskeleton during germ cell transition from mitosis to meiosis. Further experiments will be required to determine whether it localizes to an organelle in the cytoplasm of spermatogonia and spermatocytes. *Anapc10* was identified by our computational model as a meiotic candidate because of an expression profile similar to *Msh4* and *Msh5* in prophase of both males and females [22]. The prediction based on conserved coexpression does not guarantee physical interactions or functional associations. Our experimental results suggest that the coexpression link between *Anapc10* and *Msh4*/*Msh5* may reflect the concurrent processes of microtubule reorganization and recombination in meiotic prophase.

Identification of gene networks that regulate male and female meiosis is a prerequisite if we are to bridge the knowledge gap of germ cell biology. This study demonstrated that our integrative computational and experimental approach is valuable in the identification of novel meiotic genes, for which little or no information regarding meiotic function is available. In fact, *Ankrd17* and *Anapc10* could not be identified solely based on their microarray expression or similar expression profiles to *Stra8* [25]. Our approach has proven successful, as the expression and localization patterns of *Ankrd17* and *Anapc10* implicate their roles in meiotic prophase of male germ cells. Meiotic functions of these two genes will be determined by future loss-of-function studies in both males and females. Notably, though, characterizing expression and meiotic function of two candidate genes serves as a proof of concept of our approach; such studies can be performed on any candidate in a specific meiotic process. Our approach is to generate a global meiotic network before the undertaking of gene prioritization and functional characterization. The computational models also allow the identification of candidate genes that are specific to males or females and those that are common to both sexes. Therefore, the significance of this study lies not only in the expression analysis of two candidate genes, but also in the proof of concept of our computational models, which have delivered a larger candidate gene set to the broader reproductive community [22, 23, 41]. We have previously validated these models statistically by using known meiotic genes. Because of the small number of mammalian meiotic genes (~100) among genes genome-wide (~20 000), the precision of identifying known meiotic genes by random cherry picking is 0.5%. Our models have achieved up to 8-fold increase in precision compared to random cherry picking and up to 7-fold increase in precision compared to coexpression analyses of individual microarray studies [22, 23, 41]. The ultimate proof of our models would be experimentally testing a list of top-ranked candidate genes to obtain prediction accuracy. In summary, our computational models should accelerate the meiotic gene discovery process, increase our understanding of mammalian gametogenesis, and have a broad impact on reproductive research.

ACKNOWLEDGMENT

The authors would like to acknowledge Ryan Evanoff, Jun Yin, Yi Xie, and Ming-Han Tong for technical help and discussions.

REFERENCES

1. Bowles J, Knight D, Smith C, Wilhelm D, Richman J, Mamiya S, Yashiro K, Chawengsaksophak K, Wilson MJ, Rossant J, Hamada H, Koopman P.

Retinoid signaling determines germ cell fate in mice. Science 2006; 312: 596–600.
2. Koubova J, Menke DB, Zhou Q, Capel B, Griswold MD, Page DC. Retinoic acid regulates sex-specific timing of meiotic initiation in mice. Proc Natl Acad Sci U S A 2006; 103:2474–2479.
3. Bowles J, Koopman P. Retinoic acid, meiosis and germ cell fate in mammals. Development 2007; 134:3401–3411.
4. Handel MA, Schimenti JC. Genetics of mammalian meiosis: regulation, dynamics and impact on fertility. Nat Rev Genet 2010; 11:124–136.
5. Hunt PA, Hassold TJ. Human female meiosis: what makes a good egg go bad? Trends Genet 2008; 24:86–93.
6. Morelli MA, Cohen PE. Not all germ cells are created equal: aspects of sexual dimorphism in mammalian meiosis. Reproduction 2005; 130: 761–781.
7. Gerton JL, Hawley RS. Homologous chromosome interactions in meiosis: diversity amidst conservation. Nat Rev Genet 2005; 6:477–487.
8. Baker SM, Bronner CE, Zhang L, Plug AW, Robatzek M, Warren G, Elliott EA, Yu J, Ashley T, Arnheim N, Flavell RA, Liskay RM. Male mice defective in the DNA mismatch repair gene PMS2 exhibit abnormal chromosome synapsis in meiosis. Cell 1995; 82:309–319.
9. Baker SM, Plug AW, Prolla TA, Bronner CE, Harris AC, Yao X, Christie DM, Monell C, Arnheim N, Bradley A, Ashley T, Liskay RM. Involvement of mouse Mlh1 in DNA mismatch repair and meiotic crossing over. Nat Genet 1996; 13:336–342.
10. Libby BJ, Reinholdt LG, Schimenti JC. Positional cloning and characterization of Mei1, a vertebrate-specific gene required for normal meiotic chromosome synapsis in mice. Proc Natl Acad Sci U S A 2003; 100:15706–15711.
11. Ward JO, Reinholdt LG, Motley WW, Niswander LM, Deacon DC, Griffin LB, Langlais KK, Backus VL, Schimenti KJ, O'Brien MJ, Eppig JJ, Schimenti JC. Mutation in mouse hei10, an e3 ubiquitin ligase, disrupts meiotic crossing over. PLoS Genet 2007; 3:e139.
12. Bannister LA, Reinholdt LG, Munroe RJ, Schimenti JC. Positional cloning and characterization of mouse mei8, a disrupted allele of the meiotic cohesin Rec8. Genesis 2004; 40:184–194.
13. Chalmel F, Rolland AD, Niederhauser-Wiederkehr C, Chung SS, Demougin P, Gattiker A, Moore J, Patard JJ, Wolgemuth DJ, Jegou B, Primig M. The conserved transcriptome in human and rodent male gametogenesis. Proc Natl Acad Sci U S A 2007; 104:8346–8351.
14. Houmard B, Small C, Yang L, Naluai-Cecchini T, Cheng E, Hassold T, Griswold M. Global gene expression in the human fetal testis and ovary. Biol Reprod 2009; 81:438–443.
15. Lawson C, Gieske M, Murdoch B, Ye P, Li Y, Hassold T, Hunt PA. Gene expression in the fetal mouse ovary is altered by exposure to low doses of bisphenol A. Biol Reprod 2011; 84:79–86.
16. Olesen C, Nyeng P, Kalisz M, Jensen TH, Moller M, Tommerup N, Byskov AG. Global gene expression analysis in fetal mouse ovaries with and without meiosis and comparison of selected genes with meiosis in the testis. Cell Tissue Res 2007; 328:207–221.
17. Rolland AD, Lehmann KP, Johnson KJ, Gaido KW, Koopman P. Uncovering gene regulatory networks during mouse fetal germ cell development. Biol Reprod 2011; 84:790–800.
18. Schultz N, Hamra FK, Garbers DL. A multitude of genes expressed solely in meiotic or postmeiotic spermatogenic cells offers a myriad of contraceptive targets. Proc Natl Acad Sci U S A 2003; 100:12201–12206.
19. Shima JE, McLean DJ, McCarrey JR, Griswold MD. The murine testicular transcriptome: characterizing gene expression in the testis during the progression of spermatogenesis. Biol Reprod 2004; 71:319–330.
20. Small CL, Shima JE, Uzumcu M, Skinner MK, Griswold MD. Profiling gene expression during the differentiation and development of the murine embryonic gonad. Biol Reprod 2005; 72:492–501.
21. Skarnes WC, Rosen B, West AP, Koutsourakis M, Bushell W, Iyer V, Mujica AO, Thomas M, Harrow J, Cox T, Jackson D, Severin J, et al. A conditional knockout resource for the genome-wide study of mouse gene function. Nature 2011; 474:337–342.
22. Li Y, Lam KS, Dasgupta N, Ye P. A yeast's eye view of mammalian reproduction: cross-species gene co-expression in meiotic prophase. BMC Syst Biol 2010; 4:125.
23. Zheng P, Griswold MD, Hassold TJ, Hunt PA, Small CL, Ye P. Predicting meiotic pathways in human fetal oogenesis. Biol Reprod 2010; 82: 543–551.
24. Peters AH, Plug AW, van Vugt MJ, de Boer P. A drying-down technique for the spreading of mammalian meiocytes from the male and female germline. Chromosome Res 1997; 5:66–68.
25. Hogarth CA, Mitchell D, Evanoff R, Small C, Griswold M. Identification and expression of potential regulators of the mammalian mitotic-to-meiotic transition. Biol Reprod 2011; 84:34–42.
26. Watt AJ, Jones EA, Ure JM, Peddie D, Wilson DI, Forrester LM. A gene trap integration provides an early in situ marker for hepatic specification of the foregut endoderm. Mech Dev 2001; 100:205–215.
27. Forrester LM, Nagy A, Sam M, Watt A, Stevenson L, Bernstein A, Joyner AL, Wurst W. An induction gene trap screen in embryonic stem cells: identification of genes that respond to retinoic acid in vitro. Proc Natl Acad Sci U S A 1996; 93:1677–1682.
28. Ioana M, Angelescu C, Burada F, Mixich F, Riza A, Dumitrescu T, Alexandru D, Ciurea T, Cruce M, Saftoiu A. MMR gene expression pattern in sporadic colorectal cancer. J Gastrointest Liver Dis 2010; 19: 155–159.
29. Sedgwick SG, Smerdon SJ. The ankyrin repeat: a diversity of interactions on a common structural framework. Trends Biochem Sci 1999; 24: 311–316.
30. Deng M, Li F, Ballif BA, Li S, Chen X, Guo L, Ye X. Identification and functional analysis of a novel cyclin e/cdk2 substrate ankrd17. J Biol Chem 2009; 284:7875–7888.
31. Hou SC, Chan LW, Chou YC, Su CY, Chen X, Shih YL, Tsai PC, Shen CK, Yan YT. Ankrd17, an ubiquitously expressed ankyrin factor, is essential for the vascular integrity during embryogenesis. FEBS Lett 2009; 583:2765–2771.
32. Bellve AR, Millette CF, Bhatnagar YM, O'Brien DA. Dissociation of the mouse testis and characterization of isolated spermatogenic cells. J Histochem Cytochem 1977; 25:480–494.
33. Wendt KS, Vodermaier HC, Jacob U, Gieffers C, Gmachl M, Peters JM, Huber R, Sondermann P. Crystal structure of the APC10/DOC1 subunit of the human anaphase-promoting complex. Nat Struct Biol 2001; 8: 784–788.
34. Grossberger R, Gieffers C, Zachariae W, Podtelejnikov AV, Schleiffer A, Nasmyth K, Mann M, Peters JM. Characterization of the DOC1/APC10 subunit of the yeast and the human anaphase-promoting complex. J Biol Chem 1999; 274:14500–14507.
35. Thornton BR, Ng TM, Matyskiela ME, Carroll CW, Morgan DO, Toczyski DP. An architectural map of the anaphase-promoting complex. Genes Dev 2006; 20:449–460.
36. Kominami K, Seth-Smith H, Toda T. Apc10 and Ste9/Srw1, two regulators of the APC-cyclosome, as well as the CDK inhibitor Rum1 are required for G1 cell-cycle arrest in fission yeast. EMBO J 1998; 17: 5388–5399.
37. Pesin JA, Orr-Weaver TL. Regulation of APC/C activators in mitosis and meiosis. Annu Rev Cell Dev Biol 2008; 24:475–499.
38. Pravtcheva DD, Wise TL. Disruption of Apc10/Doc1 in three alleles of oligosyndactylism. Genomics 2001; 72:78–87.
39. Kurasawa Y, Todokoro K. Identification of human APC10/Doc1 as a subunit of anaphase promoting complex. Oncogene 1999; 18:5131–5137.
40. Hassold T, Hunt P. To err (meiotically) is human: the genesis of human aneuploidy. Nat Rev Genet 2001; 2:280–291.
41. Su Y, Li Y, Ye P. Mammalian meiosis is more conserved by sex than by species: conserved co-expression networks of meiotic prophase. Reproduction 2011; 142:675–687.
42. Yeo WM, Chow VT. The VP1 structural protein of enterovirus 71 interacts with human ornithine decarboxylase and gene trap ankyrin repeat. Microb Pathog 2007; 42:129–137.
43. Pines J. Cubism and the cell cycle: the many faces of the APC/C. Nat Rev Mol Cell Biol 2011; 12:427–438.
44. Herbert M, Levasseur M, Homer H, Yallop K, Murdoch A, McDougall A. Homologue disjunction in mouse oocytes requires proteolysis of securin and cyclin B1. Nat Cell Biol 2003; 5:1023–1025.
45. Kudo NR, Wassmann K, Anger M, Schuh M, Wirth KG, Xu H, Helmhart W, Kudo H, McKay M, Maro B, Ellenberg J, de Boer P, et al. Resolution of chiasmata in oocytes requires separase-mediated proteolysis. Cell 2006; 126:135–146.
46. Terret ME, Wassmann K, Waizenegger I, Maro B, Peters JM, Verlhac MH. The meiosis I-to-meiosis II transition in mouse oocytes requires separase activity. Curr Biol 2003; 13:1797–1802.
47. Magnuson T, Epstein CJ. Oligosyndactyly: a lethal mutation in the mouse that results in mitotic arrest very early in development. Cell 1984; 38: 823–833.
48. Buschhorn BA, Petzold G, Galova M, Dube P, Kraft C, Herzog F, Stark H, Peters JM. Substrate binding on the APC/C occurs between the coactivator Cdh1 and the processivity factor Doc1. Nat Struct Mol Biol 2011; 18: 6–13.